20. Molecule Microscopy

Academic and Research Staff

Prof. J.G. King, Prof. R.M. Latanision, Prof. A.P. French, Dr. A. Essig, Dr. J.A. Jarrell, Dr. S.J. Rosenthal

Research Objectives

Molecule microscopes produce images which reveal the spatial variation in the flux of molecules from sample surfaces. These molecules may be part of the bulk samples, foreign species bound to the surface, or they may permeate the samples. Desorption of the molecules by pulsed focused beams in the first two cases, with subsequent identification and detection can reveal the spatial distribution of molecules on the surface. Measurement of molecule fluxes permeating the sample reveal the spatial distribution of permeability of the sample. Our objective has been to study contrast mechanisms, devise ways of achieving adequate sensitivity and spatial resolution, design and build apparatus and use it to study interesting problems in biology and material science. Substantial progress in 1985 has been made in two projects only, one involving the Scanning Micropipette Molecule Microscope at Boston University School of Medicine and the other being the design of a Molecule Microscope for the visualization of the hydrogen permeation of metals. A proposal has been prepared in collaboration with R.M. Latanision of the Department of Material Science and Engineering for this latter project. Other proposals for continuing various parts of our program are also in preparation.

20.1 Scanning Micropipette Molecule Microscopy — in collaboration with Boston University School of Medicine

National Institutes of Health (Grant AM-25535)

Whitaker Foundation

Stanley J. Rosenthal, John G. King, Alvin Essig

We are continuing work with the Boston University instrument directed towards better performance and characterization. Our object is to reveal variations in water flow through various samples immersed in water of saline solutions. Experiments are being carried out in both a synthetic model system and in biological tissues. For studies in a synthetic model system we employ porous membranes of Nuclepore polycarbonate (Nuclepore Corporation, presently available as Uni-pore, Bio-Rad). These plastic membranes, prepared by irradiation and etching, offer many desirable characteristics for our purpose, being inert, strong, flexible, hydrophilic, yet nonhygroscopic, and with a very smooth surface, with a peak-to-valley distance of less than 0.1 μm. The pores are round, of well characterized size, and distributed randomly. Membranes are available in a large variety of pore sizes and average spacings. We mostly use membranes with a pore size of 5.0 μm and a pore density of $4 \times 10^5/cm^2$.

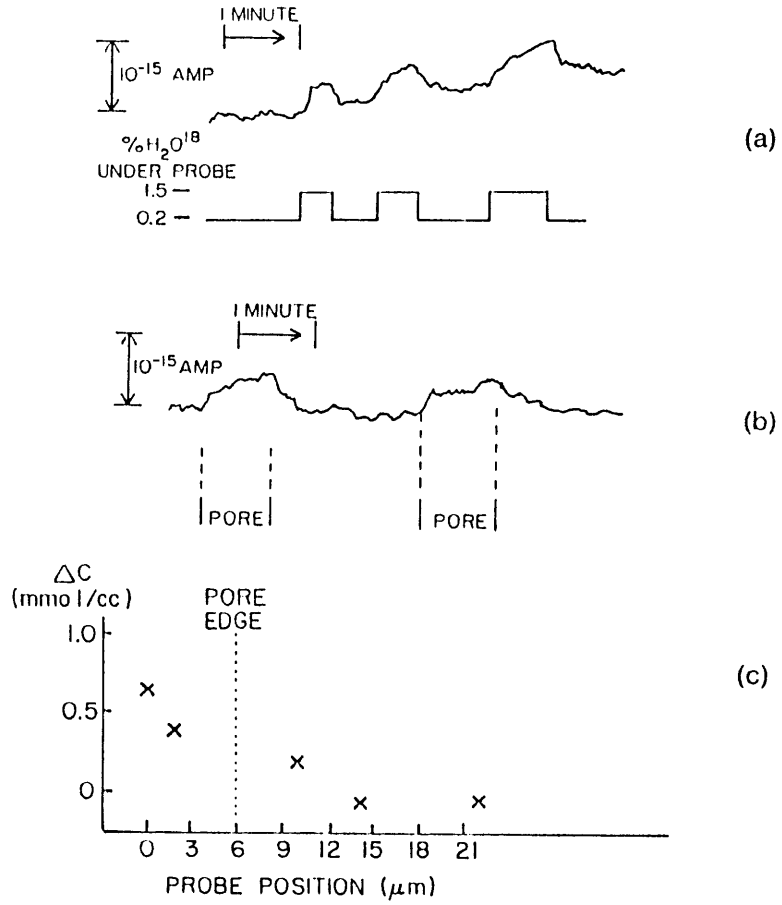

Figure 20-1: (a) The signal from a high sensitivity probe (3 μm I.D., 8 μm O.D., membrane thickness < 0.5 μm). The probe is exposed to either normal water (H_2O^{18} isotopic abundance = 0.2%) or to water containing 1.5% H_2O^{18}.

(b) Test with Nuclepore membrane, pore diameter = 12 μm. The signal is from the above probe. It is placed alternately above a pore or 15 μm from a pore. The average distance of the probe above the Nuclepore is 3 μm. H_2O^{18} flows from below at 1 x 10^{-9} l/sec.

(c) Concentration profile above single pore. The position is the horizontal distance between the probe center and the pore center. Each point is the average of 2 measurements made on opposite sides of the pore.

Probes have been scanned across these membranes and show concentration heterogeneity correlated with pore positions. These model experiments help to determine the degree of spatial resolution attainable, and to explore aspects of probe design, scanning, and other technical details in an attempt to define optimal operating conditions. Probe characteristics to be varied include tip size, taper, shape, and the nature of the glass employed. Scanning is varied with respect to distance from the membrane, as well as the rate, frequency, and extent of probe movement, in order to minimize distortion of the unstirred layer. The rate of stirring is varied in

order to determine the effect on the "unstirred layer" thickness and on the tracer concentration profile. Preliminary test results using 12.0 μm Nuclepore are shown in Fig. 20–1. Figure 20–1 is the first image of water flux through a microscopic pore.

Previously, Jarrell *et al.* have shown a similar molecular image using Helium flux.[1]

References

1. J.A. Jarrell, J.G. King, and J.W. Mills, "A Scanning Micropipette Molecule Microscope," Science, 211: 277 (1981).

20.2 Studies of Hydrogen Permeation by Molecule Microscopy

Prof. J. King, Prof. R.M. Latanision, Dr. S.J. Rosenthal
Francis L. Friedman Chair

Introduction

Hydrogen diffuses through metals along the grain boundaries and through the grains. A full understanding of these processes would certainly be relevant to the understanding and control of hydrogen embrittlement, a phenomenon of great importance in many industrial and military situations.

Though there have been many studies of hydrogen in metals going back many years, the effects of the diffusion processes have only recently been directly observed with limited spatial resolution.[1] It was found that hydrogen concentration as determined by ion microprobe analysis correlated with visible grain boundaries at a resolution of 13 μm (Fig. 20–2).
We believe that it would be valuable to achieve spatial resolution in the determination of hydrogen flux at least as good as that achieved optically (1 μm). This resolution is attainable with a simplified molecule microscope, the performance of which will guide the development of more elaborate instruments capable of resolution down to the nanometer range.

20.2.1 Hydrogen Embrittlement of Metals

As is true of other embrittlement phenomenon, hydrogen embrittlement is affected by mechanical, environmental, and metallurgical conditions. For example, the suspectability of high-strength, quench, and tempered steels to hydrogen embrittlement increases as the yield strength of the material is increased by thermal treatment. Above about 200 ksi yield strength, embrittlement occurs in moist air and water vapor. On the other hand, and with reference to environmental conditions, the presence of H_2S in aqueous environments limits the use of hardenable high-strength steel in well drilling and oil and gas production equipment to roughly 80–90 ksi yield strength. Sour gas (i.e., H_2S-containing) present substantial concern in terms of

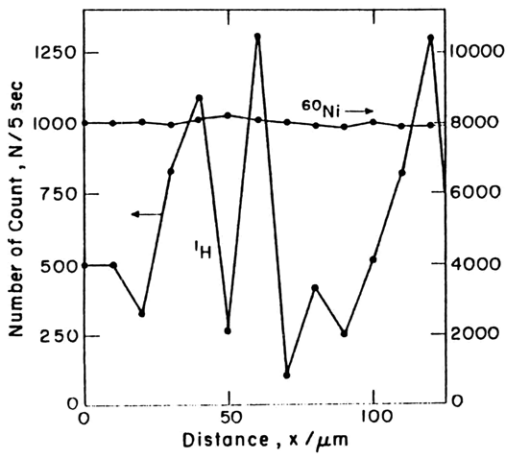

(a)

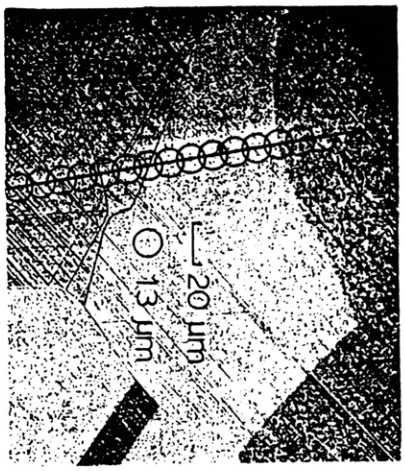

(b)

Figure 20-2: Ion Microprobe Analysis (IMA) results of Tsuru and Latanision, Reference 1.

(a) IMA data showing the increased hydrogen concentration at grain boundaries on the exit surface of a nickel specimen cathodically charged for 2 hours at the opposite or entry surface (cathode).

(b) IMA scanning direction superimposed on the optical micrograph of the surface corresponding to Fig. 20–2a. The hydrogen peaks in Fig. 20–2a correspond to grain boundary intersections.

the materials for use as tubulars in deep wells.[2] One of the most striking demonstrations of hydrogen embrittlement and its control is shown in Fig. 20–3, which illustrates the effect of oxygen, argon, hydrogen, and water on the cracking behavior of a high–strength steel.[3] Note that dry hydrogen and moisture accelerate cracking, whereas oxygen arrests crack extension. It is concluded that molecular hydrogen chemisorbs dissociatively on iron,[4] allowing atomic hydrogen

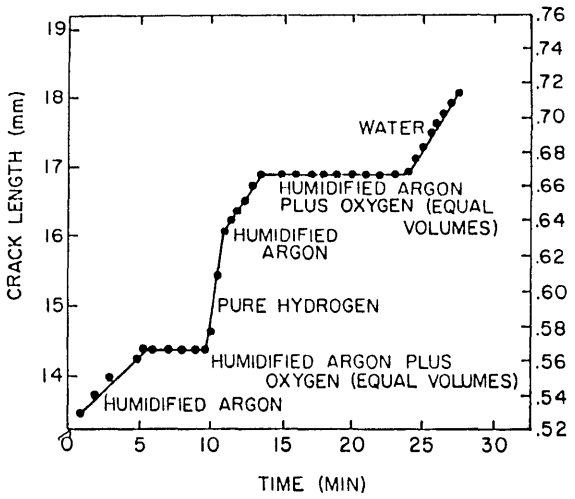

Figure 20-3: Fast crack growth of high-strength steel in water and hydrogen, but crack arrest in oxygen (after Hancock and Johnson).[3]

to be absorbed into the matrix. In moisture, it is expected that hydrogen is produced as a consequence of the corrosion of the iron surface, as explained above. In effect, whatever the source, absorbed oxygen leads to crack growth. By contrast, it is considered that oxygen inhibits embrittlement by producing an oxide barrier which suppresses subsequent absorption.

20.2.2 Mechanisms of Hydrogen Embrittlement

Hydrogen-induced losses in strength or ductility have been attributed to several mechanisms. These have been succinctly described by Louthan and McNitt,[5] and the list below is essentially an expanded version of that which appeared in their publication:

1. The accumulation of molecular hydrogen in internal voids and cracks exerts a pressure which lowers the apparent fracture stress. This *pressure model* was originally proposed by Zapffe.[6]

2. A hydrogen-induced *decohesion* of the lattice proposed by Troiano[7] and modified by Oriani.[8]

3. *Adsorption* of hydrogen to reduce the surface energy as proposed by Petch.[9]

4. Beachem's[10] suggestion that (absorbed) *hydrogen-stimulated plastic deformation* accelerated subsequent fracture. Though unspecific with regard to the means by which plasticity might be affected, recent field ion microscopy studies by Clum[11] suggests that hydrogen may reduce the work required to nucleate dislocations at the surface and, hence, induces plasticity. Lynch suggested that chemisorption facilitates dislocations at the nucleation at crack tips, although, again, the mechanism by which this should occur is not well developed.[12]

5. Formation of a hydrogen-rich phase (e.g., hydride) which has mechanical properties different than those of the matrix.[13,14] This seems quite clearly to be the case for Ti and Zr and their alloys.

6. Hydrogen-dislocation interactions which suppress glide and provide a means of producing locally large hydrogen accumulations that induce subsequent embrittlement.[14-16]

It is not intended in this instance to assess critically the above models; this has been done on many occasions by others. It seems clear that there are circumstances where some models seem to apply better than others. Considering the volume of literature which has appeared on this subject, it should be no surprise that considerable support as well as contradiction may be found for each model. It is clear, however, that important questions concerning the embrittlement process involve the location of hydrogen in metals; i.e., the possible accumulation of hydrogen at grain boundaries, the association of hydrogen with mobile dislocation, etc. There is at present no direct means of detecting hydrogen fluxes with the requisite spatial resolution to address such questions.

20.3 Molecule Microscope for H Permeation Studies: Principle in Operation

In this instrument, spatial resolution is obtained by detecting the molecules emitted from the sample with a field ionizing tip which can be scanned in a plane parallel to the sample surface at a distance of approximately 1 μm (Fig. 20-4).

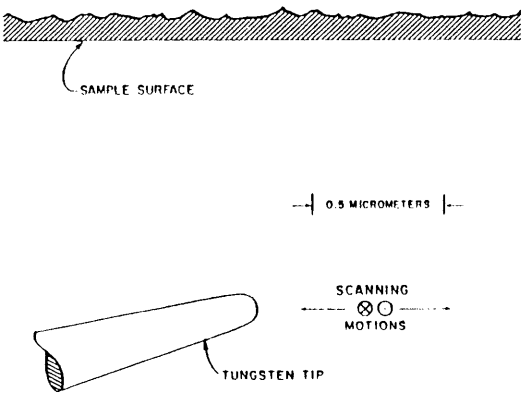

Figure 20-4: Ionizer and Sample. Field-ionizing tungsten tip approximately 0.1 μm in radius which can be scanned in a plane 1 μm from and parallel to the sample surface. Ions formed near the upper quadrant of the tip will strike the sample, producing sputtering that is entirely negligible, whereas ions formed in the lower quadrant will be detected.

The spatial resolution to be expected may be estimated on the basis of three good assumptions: molecules are emitted from a point on the sample in a cosine distribution (or narrower), the intensity falls off with the square of the distance from the emitting point on the sample, and the effective area of the detector depends on a cosine obliquity factor. Thus, the detected ion current

from the tip depends on cosine to the fourth power, and as the detector tip is scanned, the signal will fall to one-half at an angle $\cos^{-1}(0.5)^{0.25} = 33°$. Thus, the FWHM of the detected signal will correspond to moving the detector tip sideways, as distance 2 x 1 μm x tan 33 = 1.3 μm, which is the spatial resolution.

20.4 Field Ionizing Detector

The detector is an etched tungsten tip on 0.1 μm radius maintained at + 15 kv potential with respect to ground. Neutral molecules entering the region of strong electric field near the tip are ionized, and the resulting positive ions are repelled and strike the converter plate to produce secondary electrons. The negative potential of the ion deflecting plate is adjusted to maximize the detected ion current. The secondary electron current is amplified by a semiconductor electron multiplier with a gain of one million. The general arrangement is shown in Fig. 20-5. The sample is mounted on a threaded holder by soldering, welding, cementing, or other means as desired. It is then screwed vacuum-tight into a long tube and is introduced into the apparatus, ending up against a thermally nonconducting stop ring. Provisions are made for heating or cooling the sample and for gas or electrolyte behind it. The detector assembly is coarsely positioned by its mounting tube, travel being limited by three stops (two shown). Ions from the tip are attracted by the deflector plate so that they strike the converter plate and produce secondary electrons. These in turn enter the electron multiplier (gain 10^6). These four components are mounted in fixed relation on the fine adjustment and scanning motions.

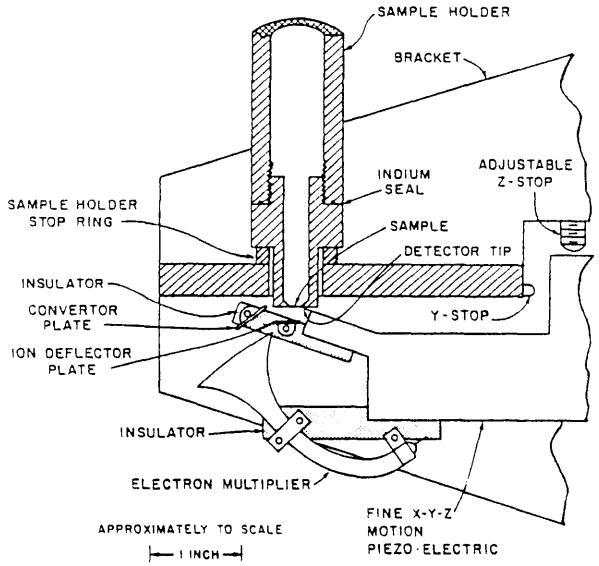

Figure 20-5: Sample and Detector Assembly

We have had extensive experience with this kind of detector in experiments where low-density fluxes of NH_3, He, and H_2O were detected. This application differs in that the tip is close to the electrically conducting surface of the sample. There are, therefore, electrostatic image forces

which will attract the tip toward the sample. Calculations show that the deflection will not be excessive and that the lowering of the natural frequency of mechanical oscillation of the tip will not make it susceptible to external vibration. Some of the ions will stride the sample, producing a negligible amount of heat and sputtering. The rest of the ions—between 30% and 50%—will strike the converter plate and produce secondary electrons. Since we are not using a mass spectrometer to analyze the ions produced, we must keep the background of more readily ionized gas in the apparatus low, as was done in our earliest work with molecule microscopy.[17] It is possible that H and H_2 could be distinguished on the basis of the difference in the ionization energies by operating the tip at different potentials.

References

1. T. Tsuru and R.M. Latanision, "Grain Boundary Transport of Hydrogen in Nickel," Scripta Met. 16, 575 (1982).
2. B.J. Berkowitz and R.D. Kane, Corrosion 36, 24 (1980).
3. G.G. Hancock and H.H. Johnson, Trans. AIME 236, 513 (1966).
4. D.O. Hayward and B.N.W. Trapnell, in "Chemisorption," 2nd edition, (Butterworths London 1964).
5. M.R. Louthan and R.P. McNitt, in Fundamental Aspects of Stress Corrosion Cracking, NACE, Houston (1969), p. 496.
6. C.A. Zapffe and C.E. Sims, Trans AIME 145, 225 (1941).
7. A.R. Troiano, Trans. ASM 52, 54 (1960).
8. R.A. Oriani, Berichte der Bunsenges fur Phys. Chem. 76, 848 (1972).
9. N.J.L. Petch, J.I.S.I. 173, 25 (1954).
10. C.D. Beachem, Met. Trans., 3, 437 (1972).
11. J.A. Clum, Scripta Met. 9, 51 (1975).
12. S.P. Lynch, Metals Forum 2, 189 (1979).
13. D.G. Westlake, Trans. ASM 62, 1000 (1969).
14. J.J. Gilman, Phil. Mag. 26, 801 (1972).
15. P. Bastien and P. Azou, Proceedings 1st World Metallurgical Congress, ASM, Cleveland (1951), p. 535.
16. J.K. Tien, A.W. Thompson, I.M. Bernstein, and R.J. Richards, Met. Trans. 7A, 821 (1976).
17. J.C. Weaver and J.G. King, "The Molecule Microscope: A New Instrument for Biological and Biomedical Research," Proc. Nat. Acad. Sci. USA 70, 2781 (1973).